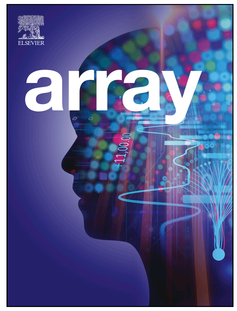

IoT Node for Monitoring and Traceability of Live Plants in Maritime Transport

Blanca Méndez, Paula Lamo

PII: S2590-0056(25)00248-6

DOI: https://doi.org/10.1016/j.array.2025.100621

Reference: ARRAY 100621

To appear in: *Array*

Received Date: 1 June 2025

Revised Date: 25 November 2025

Accepted Date: 30 November 2025

IoT Node for Monitoring and Traceability of Live Plants in Maritime Transport

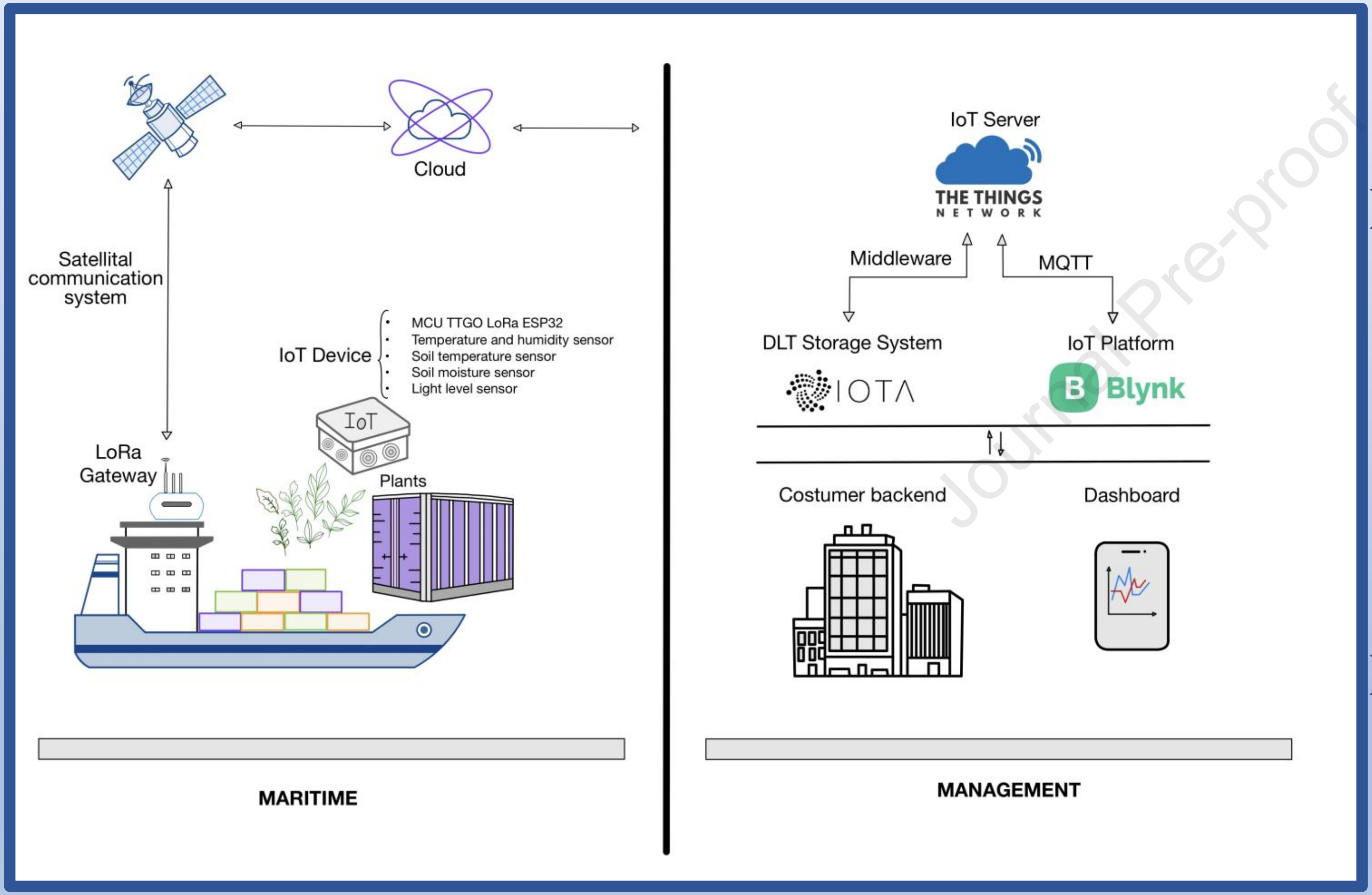

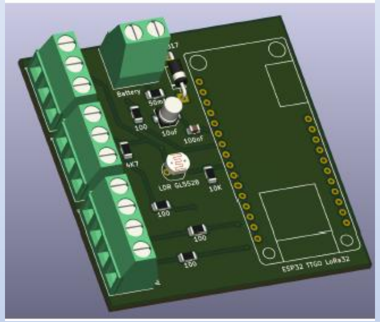

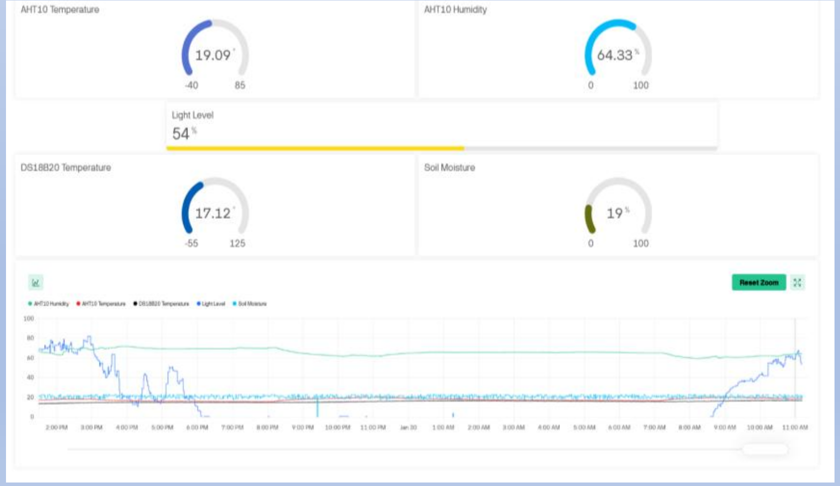

IoT Node for Monitoring and Traceability of Live Plants in Maritime Transport

Blanca Méndez[1] and Paula Lamo [1,a]

[1]Escuela Superior de Ingeniería y Tecnología, Universidad Internacional de La Rioja, 26006 Logroño, Spain

[a]Corresponding author

paula.lamo@unir.net,

KEYWORD

IOTA Tangle; Internet of Things (IoT); LoRaWAN; Maritime Monitoring Systems; Scalability Analysis.

ABSTRACT

The work presents an Internet of Things (IoT) monitoring node designed to convert shipping containers into smart greenhouses, thereby optimizing the transportation of live plants over long distances. This node utilizes specialized sensors to measure ambient temperature, soil temperature, relative humidity, soil moisture, and luminosity. Communication is via LoRa for local transmission and a low-Earth orbit (LEO) satellite infrastructure to ensure global connectivity. The collected data is stored and verified on the IOTA Tangle, ensuring traceability and immutability. Field tests in controlled environments demonstrated measurement accuracy, operational stability under varying environmental conditions, and optimized energy consumption. Additionally, the system is accessible through the Blynk platform, which provides real-time monitoring and customizable alert configurations. The paper also analyzes system costs, scalability, and specific conditions for installation on ships and containers. Limitations, such as dependence on satellite connectivity and structural barriers in maritime environments, are discussed. Finally, future lines of research focused on integrating artificial intelligence, energy optimization and connection with global logistics chains are identified.

1. Introduction

Maintaining optimal environmental conditions for live plants and agricultural products over long sea voyages is a technical challenge [1]. The viability and quality of plants depend on various factors, including temperature, relative humidity, light, and ventilation [2]. Voyages can last days or weeks. Therefore, failure to maintain these parameters within certain limits can lead to loss of goods and significant economic losses [3]. Furthermore, the technical solution must consider extreme weather conditions, extended voyage durations, and connectivity and power limitations [4].

Conventional refrigerated or ventilated containers are viable for some plants or short voyages. However, the internal configuration of containers does not allow for adequate securing of live or irregular cargo, increasing the risk of physical damage during transport. Lack of precise control over relative humidity can lead to dehydration or the proliferation of fungal diseases. Furthermore, refrigeration systems are not designed to maintain the balance of gases, such as oxygen and carbon dioxide, which can compromise plant respiration and photosynthesis. Furthermore, inadequate lighting prevents plants from continuing their metabolic processes over long journeys. This can affect their vitality. All these limitations mean that, without additional modifications such as real-time monitoring, controlled atmosphere systems, internal lighting, or stabilization mechanisms, refrigerated containers are not ideal for transporting live plants over long journeys or with specific environmental conservation requirements [2], [5].

For the communication of these monitoring systems, the special characteristics of vessels must be taken into account. Low-Power Wide Area Networks (LPWANs) [6], which operate in the sub-GHz range, can penetrate dense materials such as the steel used to construct containers and other structural elements of the vessel. Among the available options, the applicability of SigFox and NB-IoT is compromised because they depend on operator-managed networks [7], [8]. Therefore, they are not viable for maritime routes, where telecommunications coverage is minimal or nonexistent. LoRa, on the other hand, can be used on board as long as gateways or repeaters are strategically placed to ensure coverage in all areas of the vessel [9]. This system is most effective in open areas, such as decks or refrigerated containers with steel windows. However, LoRa alone cannot provide global connectivity. A practical option is to combine this solution with satellite systems to transmit data to shore. Thus, low-Earth orbit (LEO) satellites have emerged in recent years to support the development of a hybrid solution [10]. This latter combination is attractive because LoRa maintains low power consumption for onboard devices, and satellites guarantee global coverage, even in remote areas.

Furthermore, data traceability is becoming a necessity in the sector. Some current solutions include centralized blockchain-based platforms, such as TradeLens [11], which enable for the tracking of goods and environmental conditions throughout the supply chain. These platforms help build trust among logistics players, but they rely on telecommunications networks and centralized data centres, making them vulnerable to network failures or security issues [8], [12]. RFID tags have also been used, but they are limited in providing timely information and do not allow continuous or immutable data monitoring [13], [14]. In contrast, decentralized infrastructure-based solutions have begun to gain ground in maritime applications [15]. These platforms allow data to be recorded immutably and without relying on a centralized operator, ensuring information integrity even in conditions of intermittent connectivity.

This work presents a low-cost IoT node that transforms maritime containers into controlled spaces, as discussed above. The solution incorporates LoRa technology, which enables operation over long distances and exhibits low energy consumption, and IOTA [16], [17] to store and verify critical data without relying on centralized infrastructure. This guarantees the traceability of the quality of the transported plants by ensuring constant and reliable monitoring, even in extreme conditions. Furthermore, it reduces dependence on expensive and centralized solutions, making the technology accessible to small and medium-scale operators. The immutable traceability of data reinforces trust in the supply chain, allowing stakeholders to verify transport conditions in real-time. To this end, the work is structured as follows: Section 2 presents an overview of the related work. Section 3 describes the proposed IoT node, including the software, hardware, and operational functionalities. Section 4 presents the results obtained after evaluating its operation, the limitations detected, and future lines of research. Finally, the conclusions are presented.

2. Related work

Research on IoT-enabled monitoring in maritime environments has advanced in recent years, but existing efforts remain fragmented and insufficient when considered from the perspective of transporting live plants. Early approaches in cold-chain logistics for perishable foods and fisheries focused primarily on temperature and humidity logging to mitigate spoilage during extended sea voyages [18]. These systems established the value of wireless sensing combined with maritime communications, yet they largely disregarded the physiological requirements of non-refrigerated, living cargo [19]. Plants, unlike chilled fish or packaged food, demand simultaneous control of light exposure, soil moisture, gas exchange, and substrate temperature [20], [21]. The absence of studies integrating these variables creates a technological gap that compromises the viability of live cargo during transoceanic routes.

To ensure practical adoption, maritime IoT systems must comply with multiple regulatory frameworks that shape both their technical design and their operational deployment. At the international level, IMO conventions such as SOLAS establish requirements for safety at sea that indirectly reinforce the need for reliable monitoring of sensitive cargo [22]. For live-plant transport, compliance with ISO 22005 on traceability of feed and food supply chains is particularly relevant [23], as maintaining integrity of environmental data contributes directly to phytosanitary certification processes. At the communications layer, devices must conform to the European Radio Equipment Directive (RED) and associated regional spectrum regulations, which limit duty cycles and transmission power in ISM bands [24]. When extending coverage through non-terrestrial networks, integration with LEO constellations must also adhere to ITU spectrum allocations and national licensing conditions, ensuring that satellite gateways operate within authorized frequency bands [10], [25].

The communication layer has also been studied in adjacent contexts. LoRaWAN and other LPWAN standards have been tested on vessels and in port areas [26], [27], demonstrating robustness in the presence of metallic obstructions and multipath propagation. However, most implementations assume either terrestrial backhaul or shore-based gateways, overlooking the necessity of seamless integration with LEO satellites to provide connectivity on the high seas. Recent analyzes confirm that LPWAN-to-LEO hybrid architectures can deliver acceptable latencies for telemetry [28], but they have not been validated under the stringent duty-cycle and energy limitations of autonomous nodes deployed inside containers. The lack of systematic evaluation of how energy autonomy, propagation loss through steel structures, and satellite intermittency interact remains a key obstacle for practical adoption.

Parallel work on data management has emphasized centralized blockchain-based platforms to enhance traceability across logistics chains [29]. While these initiatives—exemplified by now-defunct solutions such as TradeLens [30]—highlight the importance of immutability, they expose vulnerabilities associated with reliance on centralized operators and stable broadband access. More recent studies have explored the suitability of decentralized ledgers, particularly DAG-based approaches such as IOTA, in agri-food logistics and fisheries [31], [32]. These works provide initial validation that lightweight, feeless transactions can anchor environmental telemetry to a tamper-evident infrastructure, but they stop short of addressing scalability under intermittent connectivity or constrained hardware conditions. Moreover, they do not evaluate the combined performance of ledger integration with LPWAN–satellite hybrid architectures, leaving open questions about latency, resource consumption, and failure rates in maritime contexts.

Security analyzes in maritime IoT further reveal critical gaps [33]. Existing deployments in shipping and port infrastructures have identified vulnerabilities in key management, replay protection, and data confidentiality during prolonged outages. Suggested countermeasures, such as AEAD encryption and trusted execution at gateways, have been proposed in abstract terms, but their applicability to resource-limited IoT nodes operating in deep-sleep cycles is still largely unexplored [34]. In addition, compliance studies linking IoT-enabled monitoring to international regulatory frameworks—such as ISO standards for traceability or SOLAS requirements for safety at sea—have mostly concentrated on refrigerated goods [35], [36]. These approaches neglect the particular regulatory and commercial challenges associated with live plant shipments, where environmental conditions directly affect product survival and phytosanitary certification.

Taken together, the literature provides valuable foundations in propagation modeling, LPWAN-satellite integration, decentralized traceability, and security frameworks. However, none of these domains has addressed the holistic requirements of live plant transport, where physiological, logistical, and digital trust factors intersect. The present work directly addresses this gap by proposing and experimentally validating an IoT monitoring node capable of capturing critical environmental variables, transmitting them through a LoRa–LEO hybrid architecture, and ensuring their immutable registration in the IOTA Tangle.

3. Proposed IoT monitoring system

3.1. Hardware design

The proposed system, as illustrated in Figure 1, integrates multiple technologies to ensure continuous and traceable monitoring. The design features autonomous IoT nodes equipped with specialized sensors to measure critical parameters during the transport of live plants by sea, including ambient temperature, soil temperature, relative humidity, soil moisture, and luminosity. These nodes are based on an ESP32 TTGO LoRa32 microcontroller, which integrates local processing and LoRa connectivity to transmit data over long distances with minimal power consumption. This microcontroller manages data acquisition and communication, enabling efficient control of the integrated sensors. The node's energy autonomy is achieved through a 3000 mAh Samsung INR18650-30Q lithium-ion battery, which guarantees a battery life of up to four months under typical operating conditions. This performance make possible by implementing deep sleep modes in the ESP32 firmware. The IP65-certified watertight enclosure protects the electronic components from moisture, dust, and extreme temperature fluctuations, ensuring system durability.

The sensor system (see Figure 2) includes an AHT10 for temperature and relative humidity measurement, a GL5528 LDR for light detection, and a capacitive soil moisture sensor for monitoring soil moisture levels. A DS18B20 soil temperature sensor is also used to accurately measure substrate temperature. These sensors offer accuracies of ±0.3°C and ±2% for ambient temperature and relative humidity, respectively, with an operating range of -40°C to 85°C for the AHT10 and a brightness range of 10 to 10,000 lux for the GL5528 LDR. The DS18B20, it is capable of maintaining an accuracy of ±0.5°C when operating within a substrate temperature range of -10°C to 85°C, although it can withstand temperatures ranging from -55°C to 125°C. The monitored environmental parameters were selected based on standard agronomic recommendations for ornamental and potted plants during maritime transport, as reported in previous studies and logistics guidelines, like [37], [38], [39], [40], [41]. These parameters were validated as representative for maintaining plant viability across species under controlled containerized conditions.

The node's modular design enables the integration of additional sensors tailored to the environment's specific needs, making the system adaptable to various applications, such as agricultural or maritime monitoring. This provides a flexible solution that can be configured to collect detailed environmental information tailored to the conditions of the installation site.

The node transmits the collected data via LoRa to a gateway, which acts as a hub and link between the nodes and the rest of the system. This gateway receives the LoRa transmissions from the nodes and sends them to the middleware via a local or remote connection without directly involving the satellite system. LoRa communication enables efficient coverage in closed environments, such as ships and metal containers, provided the gateway is strategically located to minimize structural barriers and ensure signal reception.

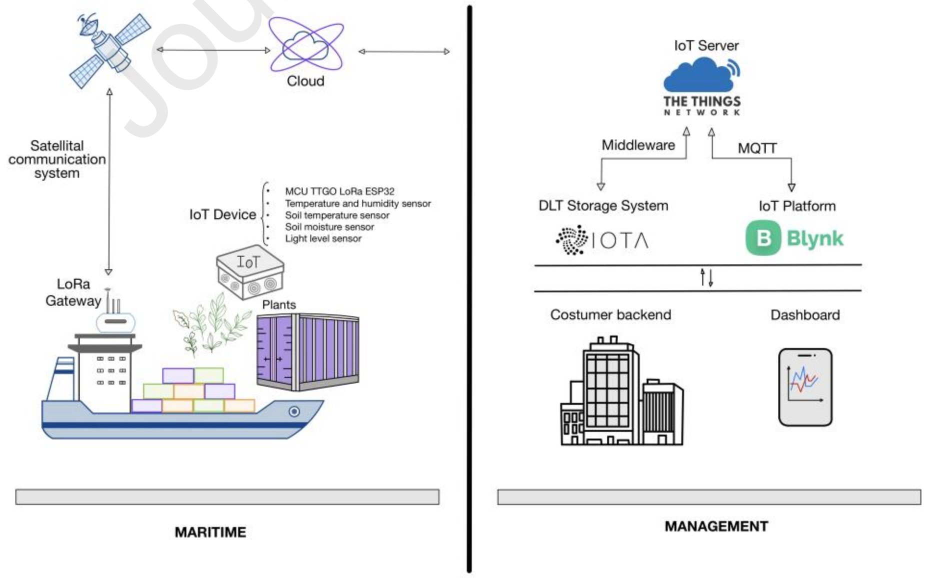

Figure 1. Proposed system architecture for monitoring live plants during maritime transport. The left section shows the maritime layer, where IoT nodes communicate via LoRa to an onboard gateway and

through satellite or cloud links. The right section represents the management layer, integrating The Things Network, IOTA for distributed data storage, and Blynk for visualization on the user dashboard.

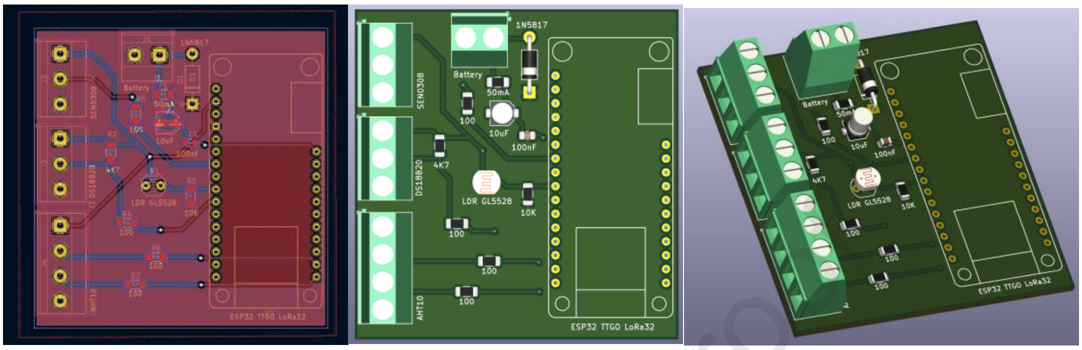

Figure 2. Printed circuit board design of the IoT node, showing the routing layout (left), the top view with main components (center), and the 3D assembly view (right).

3.2. Software implementation

When a satellite system is required, the gateway does not connect directly to the satellites. Instead, it transmits the information to the local middleware, which manages the transmission to the satellite infrastructure. This ensures that the collected data is managed efficiently, temporarily stored in case of connectivity interruptions, and finally sent to remote servers via the satellite link. This flow ensures that data integrity and global availability are guaranteed, even in environments where terrestrial connectivity is limited or nonexistent, thanks to the system's redundancy and traceability. It also prioritizes transmitting critical data and ensures its integrity through advanced encryption mechanisms. Communication between the middleware and the remote monitoring platform utilized the MQTT protocol, renowned for its low latency and efficiency in limited-bandwidth networks.

The remote monitoring platform is built on Blynk, a solution that enables users to interact with data in real-time through web-based and mobile interface (see Figure 3). This platform facilitates the visualization of measurements collected by IoT nodes. It allows configuring custom alerts based on specific thresholds for environmental parameters such as temperature, relative humidity, and brightness. These alerts notify users of critical events, enabling them to make proactive decisions.

In addition to continuous monitoring, the system integrates an alert mechanism designed to notify operators of abnormal conditions. At the device level, the IoT node provides local alerts through visual indicators when thresholds for temperature, humidity, or soil moisture are exceeded. On the cloud side, the web platform enables configurable thresholds so that critical values trigger notifications displayed directly in the user interface. This dual alert mechanism complements the monitoring function by providing both immediate feedback at the sensor node and remote visibility during maritime transport. The current architecture also leaves open the possibility of extending alerts to push notifications or email services, ensuring timely awareness for stakeholders throughout the logistics chain.

The platform includes tools for historical data analysis, enabling the identification of patterns and trends that optimize the management of the monitored environment. The data is presented in interactive graphs and tables, facilitating both interpretation and detailed analysis for end-users and technical operators. Table 1 presents the recommended recording times for transporting live plants.

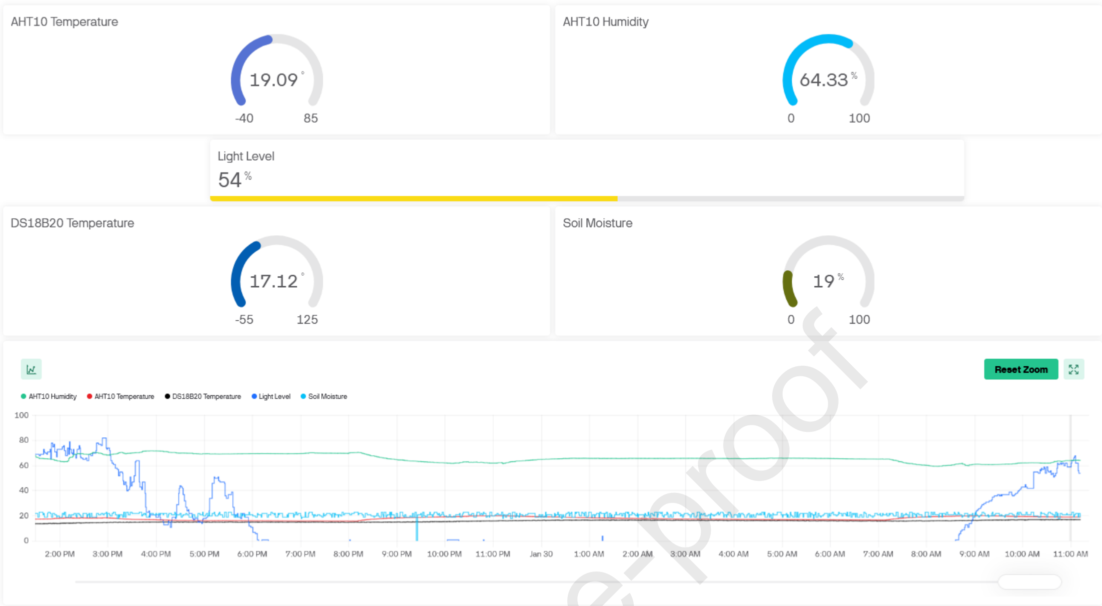

Figure 3. Dashboard of the implemented IoT platform displaying real-time measurements of ambient temperature, humidity, soil temperature, soil moisture, and light intensity. The lower panel shows the time evolution of these parameters collected by the IoT node during the monitoring period.

Table 1. Recommended registration times for environmental data logging.

Logging frequency	**Logs per day**	**Logs per month (30 days)**	**Advantages**	**Disadvantages**
Every 1 minute	*1,440*	*43,200*	*High accuracy in capturing rapid fluctuations and critical events.*	*High data volume; may be excessive for slow variations.*
Every 5 minutes	*288*	*8,640*	*Balanced trade-off between sampling frequency and storage; suitable for continuous monitoring.*	*May miss rapid events; still significant storage requirements.*
Every 15 minutes	*96*	*2,880*	*Appropriate for slow variations in the environment; lower storage demand.*	*Poor sensitivity to rapid changes in environmental conditions.*
Every 1 hour	*24*	*720*	*Suitable for stable environments with few significant variations.*	*Reduced awareness of critical event; limited analytical detail.*
Every 4 hours	*6*	*180*	*Ideal for long-term monitoring in highly stable environments.*	*Minimal ability to detect transient events.*

The data collected by IoT nodes is stored in the IOTA Tangle, a decentralized infrastructure that guarantees the immutability and traceability of the information. This storage ensures that the recorded data can be verified at any time, preventing tampering and reinforcing trust in the system. Integration with the Tangle also allows for transparent auditing of the quality of the recorded environmental conditions.

The implemented encryption layer is based on the Fernet specification, which combines AES-128 in CBC mode with HMAC-SHA256 for message authentication. A symmetric key is dynamically derived from an environment-defined counter-password concatenated with a random salt, ensuring key uniqueness and resistance to brute-force or replay attacks. The key is used to encrypt the sensor data payload prior to transmission to the middleware and subsequent storage in the IOTA Tangle. The encrypted binary output is encoded in Base64 format to maintain ASCII compatibility across heterogeneous communication channels. This mechanism provides confidentiality during data transmission and integrity verification through cryptographic signing, preventing tampering or exposure even under intermittent connectivity and constrained maritime network conditions. Although the encryption and encoding processes introduce a slight overhead in packet size, this cost is acceptable considering the enhanced data protection and traceability achieved across the full acquisition chain.

Furthermore, the system is designed to operate with low latency, even in environments with limited connectivity, thanks to the use of the MQTT protocol for communication between the monitoring platform, middleware, and IoT nodes. In the event of satellite communication loss, sensor data are stored locally in non-volatile memory until connectivity is restored. Once the link is re-established, the node automatically uploads the buffered records in chronological order through the LoRa gateway, ensuring data integrity and continuity in the distributed ledger. This ensures a fluid and reliable user experience in critical applications. It is also designed to be scalable, supporting multiple IoT nodes that can operate simultaneously without compromising performance. This capability enables deployment on vessels of various sizes and configurations. Furthermore, integration with satellite systems allows operators to receive real-time updates on transport conditions, even in geographically isolated areas.

The monitoring platform enables the dynamic adjustment of sampling and transmission frequencies, optimizing the balance between accuracy and energy consumption according to the specific needs of each route. To evaluate the energy performance of the IoT node, the average energy consumption per duty cycle was computed from direct current measurements during both active and inactive periods. The following expression was used:

$$E_{avg} = \frac{(I_{active}T_{active}) + (I_{inactive}T_{inactive})}{T_{total}} \tag{1}$$

where I_{active} and $I_{inactive}$ are the currents measured during active and inactive modes, and T_{active}, $T_{inactive}$, and T_{total} are the corresponding time intervals within one operational cycle. This empirical formulation provides a representative estimate of the node's energy behavior based on experimental data rather than a theoretical battery model.

3.3. LoRa network coverage

The effective range of a LoRa signal depends on the characteristics of the transmitter, receiver, and environmental conditions. To determine its range and design its installation on the vessel, it is necessary to consider its structural characteristics and the propagation conditions within the environment. The equation that defines coverage is

$$R = \frac{P_t + P_r}{L + G} \tag{2}$$

where R is the signal range, P_t the transmission power of the IoT node, P_r the receiver sensitivity at the gateway, L the channel loss, including interference and obstacles, and G the system antenna gain.

Shipping containers are primarily made of steel, which introduces signal propagation losses due to their high density and ability to block radio frequency signals. This increases channel losses, which can vary between 20 and 40 dB, depending on the steel thickness, the number of walls traversed, and the positioning of the node within the container. Signals inside the vessel must pass through more complex structures, such as metal compartments, multiple decks, and electromagnetic equipment, which generate additional interference. For evaluation purposes, Table 2 compares typical design values that are consistent with several studies that have characterized LoRa propagation in maritime or metallic environments, like [42], [43], [44].

Table 2. Typical theoretical parameter values and link budget margins for LoRa coverage in different ship environments.

Location	P_t [dBm] *(range: 14 - 20)*	P_r [dBm] *(range: -130 - -137)*	L [dB]	G [dB] *(standard antenna, range: 2 - 5)*	R [dB]	Conditions
Inside a shipping container	*14*	*-137*	*30 (metal walls, range: 20 - 40)*	*2*	*4.52 (viable but with limitations)*	*Significant losses from dense metal walls; viable with optimized node placement near openings and gateway outside the container.*
Inside the ship (example of engine room)	*14*	*-137*	*50 (electromagnetic interference, range: 40 - 60)*	*2*	*3.02 (weak coverage)*	*High electromagnetic interference and multiple metal barriers; most challenging scenario.*
Inside the ship (example of cargo area)	*14*	*-137*	*40 (moderate structures, range: 30 - 50)*	*2*	*3.68 (moderate)*	*Intermediate environment with moderate metal structures; acceptable with well-positioned gateways*
Clear deck	*14*	*-137*	*5 (minimal losses, range: 2 - 10)*	*5*	*9.13 (excellent coverage)*	*Minimal obstacles and optimal propagation conditions.*

3.4. System costs

The cost analysis of the proposed system is based on the unit prices of the components that make up the IoT nodes and the additional elements required for their operation at different installation scales. The cost of each IoT node, including the main components, was estimated at USD 88. This value considers the ESP32 TTGO LoRa32 microcontroller with antenna (USD 31), the AHT10 sensor (USD 2), a GL5528 LDR (USD 0.20), the SEN0308 sensor (USD 17.50), and the DS18B20 sensor (USD 2.10). In addition, a Samsung INR18650-30Q lithium-ion battery (USD 7.50), an IP65 waterproof case (USD 16), and other minor accessories, such as cables and connectors (USD 11), were included. For network management, the system requires LoRa gateways (USD 275). The number of gateways required depends on the size of the installation and the specific environmental conditions. Therefore, the total system cost, expressed as a function of the number of nodes and gateways required, is:

$$C = NC_n + G_L C_g \quad (3)$$

where C is the total cost, N the number of IoT nodes, C_n the cost per node, G_L the number of gateways required, and C_g the cost per gateway.

For vessels that do not have satellite communications previously, and this component needs to be budgeted, the total cost of the system with satellite integration, including both the physical elements and operating costs, is:

$$C_{sat} = C + SC_S + MC_m \tag{4}$$

where C_{sat} is the total system cost including satellite integration, S the number of satellite terminals multiplied by their unit cost C_s, and M the amount of data transmitted monthly multiplied by the transmission cost per megabyte C_m.

Beyond the initial investment in hardware and the operating costs of satellite connectivity, the long-term economic viability of the system is determined by its total cost of ownership (TCO). This includes maintenance costs derived from the maritime environment, such as periodic calibration or replacement of sensors exposed to humidity and salinity, as well as the eventual replacement of lithium-ion batteries after their expected service life. Operational costs also arise from hosting and maintaining the cloud platform, implementing security updates, and providing technical support to ensure system availability. These recurring costs, although lower than the initial hardware expenditure on a per-node basis, accumulate over the system lifetime and must be considered when assessing competitiveness with respect to manual monitoring practices. By incorporating these elements, the cost model provides not only a scalable estimate of initial deployment but also a realistic perspective on long-term sustainability.

To reflect the long-term economic viability of the system, the model can be extended to include operational and maintenance costs in addition to the initial hardware and satellite expenditures. The total cost of ownership over a time horizon T is expressed as

$$C_{tot} = C_{sat} + T(C_{op} + C_{maint}) \tag{5}$$

where C_{op} represents recurring operational expenses (e.g., cloud hosting, software updates, and technical support), and C_{maint} represents maintenance costs (e.g., sensor calibration, replacement of corroded components, and battery substitution).

This model allows costs to be dynamically adjusted according to the facility's size and needs. These values reflect the impact of scale on total cost, highlighting the importance of optimizing the number of gateways based on the required coverage. In a small network with few nodes and low data consumption, the operating term will have a lower impact. In larger networks or with high transmission frequencies, the term associated with data consumption becomes more relevant.

3.5. Testing protocols

The evaluation of the proposed monitoring system was conducted through a structured procedure that included calibration of each sensor, controlled data acquisition campaigns, and statistical validation.

The AHT10 sensor for ambient temperature and relative humidity was validated against a calibrated thermo-hygrometer (±0.1 °C, ±1 % RH). The procedure included a 10-minute stabilization period, followed by 60 minutes of simultaneous measurements at two controlled setpoints (23 °C, 50 % RH and 30 °C, 70 % RH). Readings were logged at 1-minute intervals. The DS18B20 soil temperature probe was validated against a laboratory thermometer with a resolution of ±0.1°C, using the same stabilisation and logging procedure. The SEN0308 capacitive soil moisture sensor was calibrated by a two-point method: insertion into oven-dried substrate (0 % reference) and into fully saturated soil (100 % reference). The raw ADC values were mapped linearly to a 0–100 % scale. The GL5528 LDR was characterized as a relative indicator of illumination by recording ADC values under dark (<10 lux), medium (≈300 lux), and bright (>3000 lux) conditions, and verifying a monotonic response against a handheld luxmeter (accuracy ±5 %).

Calibrated nodes were deployed in representative maritime environments, including inside a shipping container, the engine room, the cargo area, and on the open deck. Each node transmitted data to a LoRa gateway placed to minimize structural barriers. Where satellite integration was required, the gateway relayed messages through the middleware to the satellite terminal. Sampling intervals of 1, 5, 15, 60, and 240 minutes were tested (Table 1).

Power-consumption characterization was carried out using a precision ammeter and oscilloscope to capture the current profile during one complete acquisition cycle. Measurements included wake-up, sensor activation, LoRa transmission, and standby periods. These data were used to derive the average current in active and sleep modes, enabling later estimation of energy autonomy as a function of sampling interval.

Calibration datasets were analyzed to compute mean offsets and 95 % confidence intervals based on Student's t-distribution. Residual normality was assessed using the Shapiro–Wilk test. When normality was confirmed, paired t-tests were applied to compare sensor and reference values; otherwise, the Wilcoxon signed-rank test was used. This statistical protocol was applied consistently across all sensor datasets prior to deployment tests.

4. Results

The node was tested in a controlled environment replicating agricultural conditions in a shipping container transporting live plants, with artificial lighting and fluctuations in temperature and humidity (see setup in Figure 4). One thousand four hundred forty daily records (one per minute) were continuously monitored over 30-days period, generating 43,200 measurements. All data were manually verified, and consistency in measurements and storage was demonstrated. Sending data every minute in this type of installation may be excessive in practice, but it was assumed to be a reasonable time to evaluate the robustness of the installation.

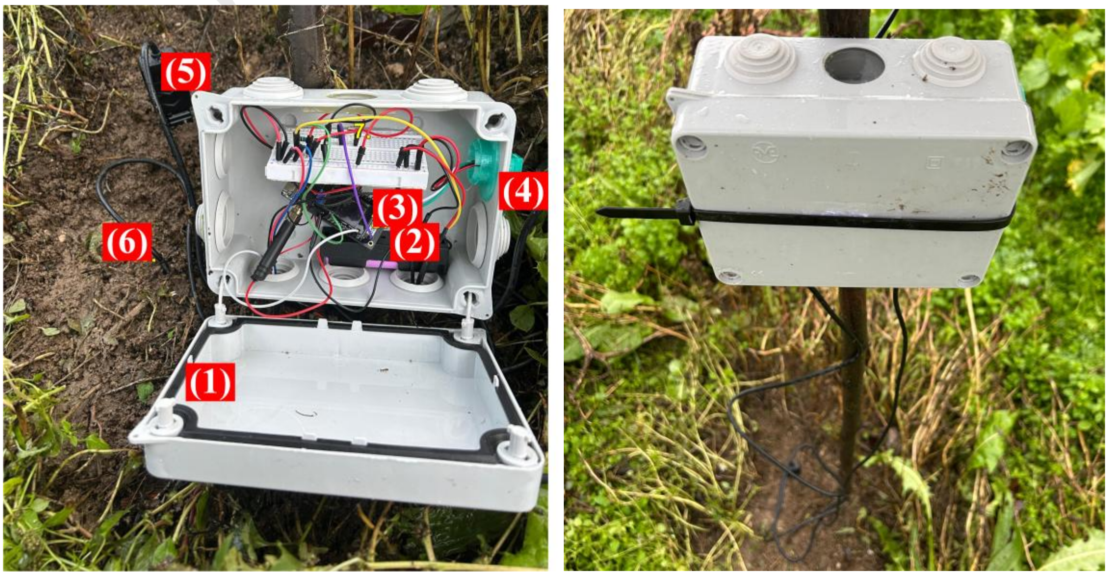

Figure 4. Tested prototype whose components are 1) IP65 waterproof box, 2) Samsung INR18650-30Q battery and battery holder, 3) ESP32 TTGO LoRa32 microcontroller with its LoRa antenna, 4) AHT10 sensor, 5) SEN0308 sensor, 6) DS18B20 sensor and 7) LDR GL5528 sensor.

4.1.Accuracy in data collection

The IoT node demonstrated accurate results during data collection tests. Environmental parameters were continuously monitored to assess their stability and variability during data processing. The plants were exposed to controlled temperature, humidity, and luminosity conditions, and data were sampled every minute, processed, and sent to the Tangle to ensure secure and consistent storage.

Temperature measurements had a margin of error of ±0.3°C over an operating range of -40°C to 85°C. For relative humidity, the margin of error was ±2% over a range of 0% to 100%. The LDR luminosity sensor recorded consistent values with optimal sensitivity in illumination ranges of 10 to 10,000 lux, allowing light variations to be assessed under low- and high-intensity conditions. Below is an example of a stored block ID corresponding to a transaction:

0x1e95ee2af6419b846d7c63f7be6236e0391d895752209d87ab02ac883e02eacf

The node maintained stable operation under controlled variations in ambient temperature and humidity. The device was subjected to temperature cycles ranging from 15°C to 20°C and relative humidity levels between 59% and 72%. The performance of the microcontroller and sensors was unaffected, and the collected data was successfully stored in local memory without any loss of information.

The ESP32 microcontroller can be configured with a 4 MB Flash memory, which allows for the storage of up to 50,000 data records in JSON format. Testing demonstrated that the node can operate without external connectivity, accumulating data locally for later transmission.

One of the key aspects evaluated was the processing time per record, from its publication on The Things Network's global network to the confirmation of its storage in the IOTA Tangle. The average processing time per record was determined to be 1.04 seconds, with a standard deviation of 0.52 seconds, indicating variability in system performance.

The data in Figure 5 reflect measurements obtained during continuous monitoring, where the plants were exposed to moderate and constant environmental conditions representative of their growing environment.

These values show that environmental parameters remained within consistent ranges overall, ensuring homogeneous conditions during data sampling. However, significant differences in luminosity were observed, with an extensive range suggesting significant variations in light exposure throughout the day.

Regarding processing time, while the average of 1.04 seconds suggests stable performance, the maximum of 4.58 seconds indicates that significant delays may occur under certain conditions, possibly due to network overload on the IOTA Tangle.

Across the 43,200 measurements collected, the average deviation of temperature with respect to reference sensors was 0.18 °C (95% CI: ±0.25 °C), and for relative humidity, the mean error was 1.7% RH (95% CI: ±2.1%). Paired t-tests confirmed that these deviations were not statistically significant ($p > 0.05$). Soil moisture readings showed slightly higher dispersion, but the Wilcoxon signed-rank test indicated that deviations were not significant at the 5% level. These findings confirm that the measured accuracy is consistent with sensor specifications and suitable for monitoring under maritime conditions.

4.2. Analysis of processing times

In detail, the box-and-whisker plot in Figure 5 represents the distribution of processing times per record. It reveals a distribution with a central tendency but with outliers that indicate occasional variability in system performance.

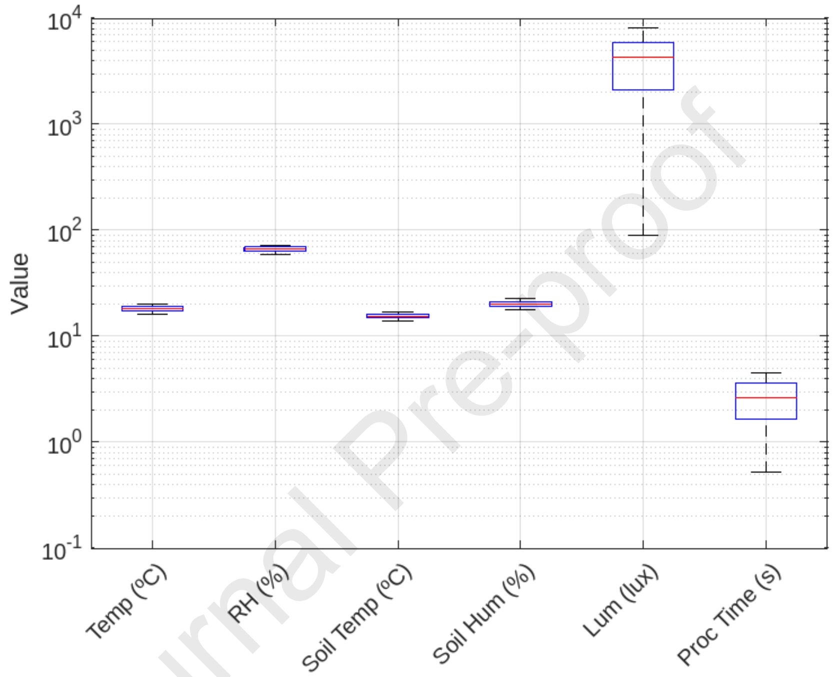

Figure 5. Boxplot representation of continuous measurements collected by the IoT node for ambient temperature, relative humidity, soil temperature, soil humidity, light intensity, and processing time. The plot summarizes the variability and dispersion of each parameter during the monitoring period.

The graph shows that the interquartile range (IQR)—the blue box—is approximately between 0.8 and 1.2 seconds, indicating that 50% of the processed records fall within this range. The median, located around 1 second, confirms that most values tend to concentrate within this range, suggesting consistent and predictable performance under normal operating conditions.

On the other hand, outliers are detected at the upper end of the distribution, reaching processing times of up to 4.58 seconds. This positive skewness (skew to the right) indicates that processing time can increase significantly under certain circumstances. These values are explained by potential network saturation and overload during high traffic within the IOTA Tangle, resulting in delays in confirming data storage.

The standard deviation of 0.52 seconds indicates that, although processing is primarily stable, there are occasional fluctuations.

The system exhibits primarily stable performance, with response times concentrated around 1 second. The identified outliers suggest the possibility of congestion on the Tangle network, which can lead to latency spikes during periods of high demand. The system can perform autonomously and efficiently, even without external connectivity.

4.3. Energy efficiency

During testing, the average power consumption was 1 mA in sleep mode and 14 mA during the sampling and transmission intervals. With a sampling frequency of once every 12 hours, the node's projected battery life amounted to 4 months of continuous operation. As the sampling times increase, the battery life also increases. Thus, if only one monitoring cycle is performed daily, i.e., once every 24 hours, the battery life reaches 8 months (see equation (1)).

Figure 5 illustrates various aspects of the IoT node's energy and operational behaviour during a complete work cycle, analyzing how the cycle stages are distributed and how the system's energy resources are managed to ensure efficient operation. Figure 6.a shows the overall potential difference of the node during two complete work cycles, each lasting approximately 16.25 seconds. Figure 6.b details the energy behaviour during the initial stages of the cycle, which include the microcontroller's exit from deep sleep mode, sensor and OLED display initialization, and the initial LoRa transmission to join the network. These stages generate considerable consumption peaks, particularly when connected to the LoRa network. Figure 6.c analyzes the intermediate stages of the cycle, which include sensor readings, data payload preparation, and their transmission over the LoRa network. Figure 6.d focuses on the stage where the payload receipt confirmation is processed, and the information on the OLED display, including the TTGO, is updated. This event ensures synchronization and correct data transmission in the event of errors or interruptions. Finally, Figure 6.e illustrates the final stages of the cycle, which include updating values on the OLED display, the microcontroller's transition to low-power mode, and its permanence in this state until the beginning of the next cycle. This period of inactivity represents the majority of the cycle time and is essential for optimizing the energy autonomy of the IoT node.

4.4. IOTA scalability

The IOTA scalability tests evaluate the system's capacity to process an increasing number of IoT nodes and their associated data volume while maintaining communication and storage consistency. Three experimental tests were performed in a controlled environment with 50, 70, and 100 simulated nodes. Performance was measured from data publication in The Things Network to confirmation of storage in the IOTA Tangle. Each test executed 50 transactions (one every 10 s), each containing a sensor data block from every node. It was executed using Python scripts modeling the interaction between IoT nodes and the IOTA network. Input parameters were the number of devices (50–2000), transaction rate per node (2–10 tx s^{-1}), and network latency for terrestrial (50 ms) and satellite (500 ms) communication. The system reliability was evaluated through repeated functional tests simulating intermittent maritime connectivity. During these tests, the nodes maintained continuous data acquisition and synchronized buffered records with the ledger once the link was restored. Reliability was characterized as operational robustness, ensuring data persistence and integrity under communication interruptions.

The first test (50 nodes) yielded an average response time of 0.91 seconds (Figure 6.a), with most transactions completing under 1 second. However, isolated peaks exceeded 2 seconds, likely due to transient network congestion. The second test (70 nodes) showed increased variability, with an average latency of 1.14 seconds (Figure 6.b). Response times ranged between 0.5 and 3 seconds, accompanied by sporadic latency spikes attributed to network congestion and external delays. Besides, the third test (100 nodes) demonstrated an average latency of 0.99 seconds (Figure 6.c), reflecting a 0.08-second increase over the 50-node test but a 0.15-second reduction compared to the 70-node scenario. Notably, high-latency outliers became more frequent, reaching over 3.5 seconds.

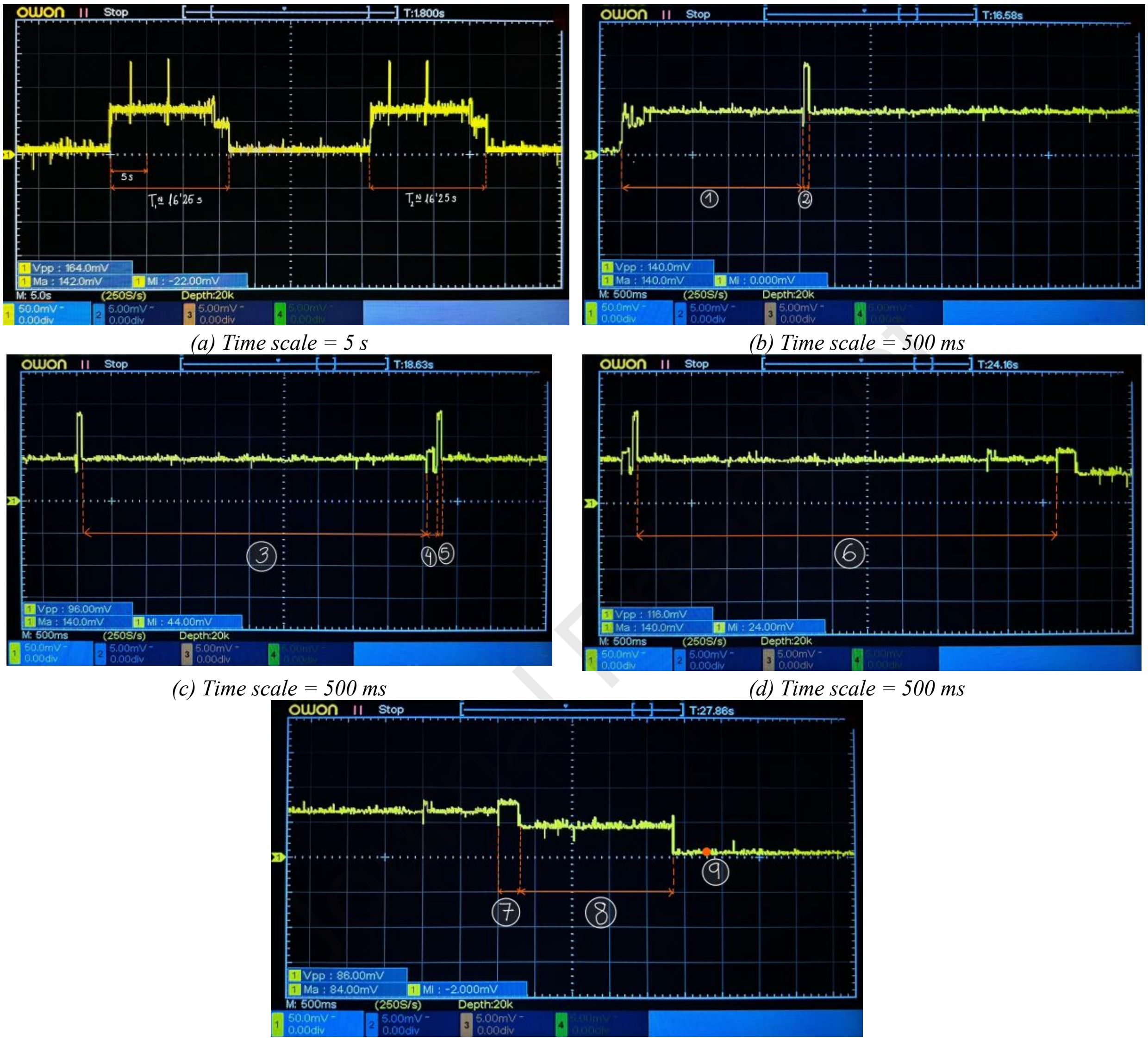

(a) Time scale = 5 s

(b) Time scale = 500 ms

(c) Time scale = 500 ms

(d) Time scale = 500 ms

(e) Time scale = 500 ms

Figure 6. Energy and operational behaviour of the IoT node during a complete cycle, where a) shows the global potential variation during two work cycles, b) illustrates the initial stages, including the exit from deep sleep mode (1), sensor initialization and the initial Lo-Ra transmission (2), c) presents the intermediate stages of the cycle, such as sensor reading (3), preparation (4) and payload transmission (5), d) details the processing of the receipt confirmation and the update of the OLED display (6) and e) shows the final stages, where the node updates the values on the OLED display (7) and enters low power mode (8) until the next cycle (9).

The results indicate that IOTA latency does not scale linearly with the number of IoT nodes. Instead, performance is influenced by factors inherent to the Tangle architecture and network dynamics. Key contributors to this non-linearity include Tangle validation and public node congestion.

Additionally, a simulation has been developed that models the scalability and performance of IoT systems, evaluating aspects, such as transaction confirmation latency in the Tangle, resource consumption, energy usage, and failure rates in a controlled environment. The conditions under which this test is executed involve simulating different node networks that could be deployed on the vessel, comprising 50, 500, 1000, and 2000 nodes. This approach enables us to assess how the system's performance changes as the number of devices increases. The rate of transactions per second per device is set to vary between 2 and 10 transactions per second and is simulated using an exponential distribution (Poisson). This parameter directly influences the volume of data the devices send to the network, affecting latency and resource consumption. The simulation time is 3600 seconds (1 hour), simulating the system behaviour in a defined period.

Additionally, this model simulates two modes of communication: satellite or terrestrial, which directly impact the latency of transactions and network coverage for the nodes. This influence is modelled by measuring the satellite coverage probability and the latencies associated with satellite (500 ms) and terrestrial (50 ms) communication. Therefore, the total latency of each transaction is calculated by summing the proof-of-work (PoW) time, the network latency (whether satellite or terrestrial), and the IOTA consensus time. For each device configuration and transaction rate, the average commit latency is calculated, which is the average time it takes for a transaction to commit to the Tangle. In addition, CPU and RAM resource modelling is performed on the IOTA nodes, distinguishing between light nodes (which require fewer resources) and Full Nodes (which require more resources). The use of these resources increases as the number of devices and the transaction rate increase. Finally, the energy consumption is calculated to reflect how network activity influences the overall energy consumption and the failure rate that can occur due to committed transactions being affected by network congestion. This rate increases when the network is highly congested, which is reflected in the competition for transaction validation in the Tangle.

The results for this simulation are presented in Figure 7.a, showing latency versus scalability. It shows the transaction confirmation latency (in milliseconds) as a function of the number of IoT devices and the transaction rate per device. In this case, the latency remains relatively stable, at around 214 ms, even with an increase in the number of devices and transactions per second. This suggests that IOTA handles scalability well in high node-density environments.

Besides, CPU Load in an IOTA node (Figure 7.b) shows the CPU usage (in percentage) on an IOTA node as a function of the number of devices and the transaction rate. It is observed that the CPU usage increases non-linearly with the number of devices, reflecting the computational load of the Tangle in validating transactions in a dense network. The higher the number of transactions per device, the higher the CPU usage increases significantly, reaching a saturation peak (130% of CPU usage) when combining 2000 devices and six transactions per second. Note that. Although the CPU may saturate, the commit latency remains stable.

RAM load in the IOTA node is shown in Figure 7.c. This result evaluates the RAM usage in megabytes in IOTA nodes, based on the number of devices and the transaction rate. RAM usage is observed to behave similarly to CPU usage; therefore, the higher the transaction rate per device, the higher the RAM usage increases, reaching a saturation peak at the combination of 2000 devices and six transactions per second. Although RAM saturates, the latency remains stable. It is worth nothing that Light Nodes consume fewer resources than Full Nodes, so it is advisable to use them or limit the transaction rate to a maximum of 6 transactions per second to prevent saturation situations.

Figure 8 presents energy consumption in the IoT system with IOTA. The system's energy consumption (in millijoules) is analyzed as a function of the devices and the transaction rate. In this case, energy consumption increases linearly with both parameters with a moderate scale factor.

Additionally, Figure 7 illustrates the impact of congestion on the IOTA on board. The failure rate caused by congestion is studied as a function of the number of devices and the transaction rate. It is observed that the failure rate increases by up to 14% in large-scale scenarios (i.e., 2000 devices with 10 transactions per second), reflecting a limitation of the Tangle under a dense data load. Therefore, it would be advisable to limit the transaction rate.

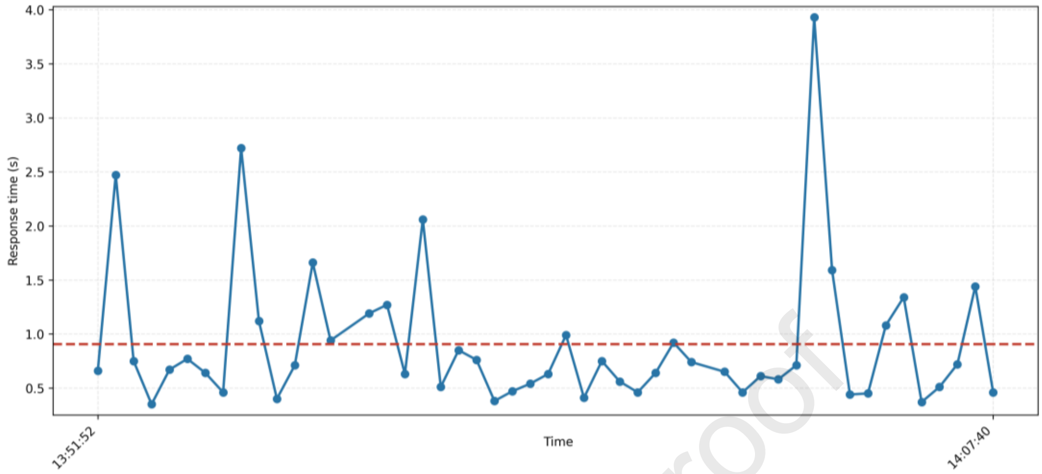

(a) Response time for 50-node transactions. Mean value = 0.91 s (in red).

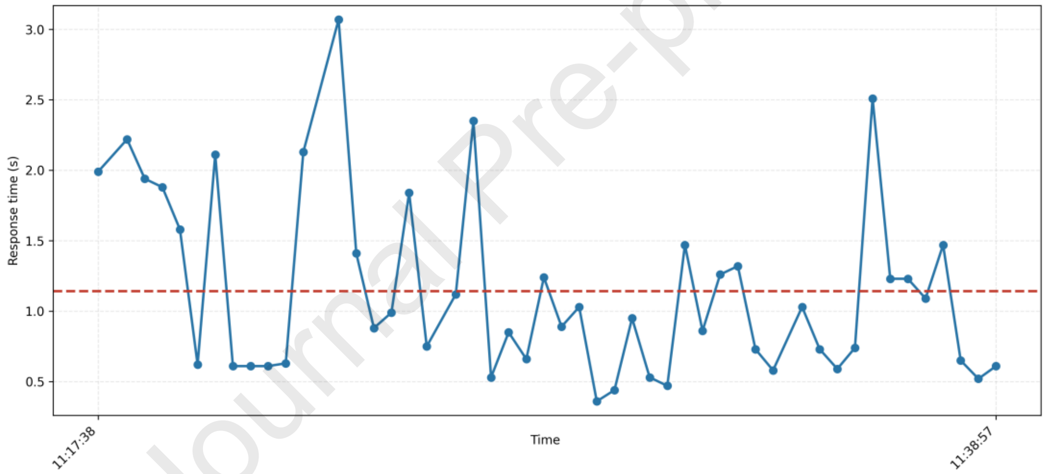

(b) Response time for 70-node transactions. Mean value = 1.14 s (in red).

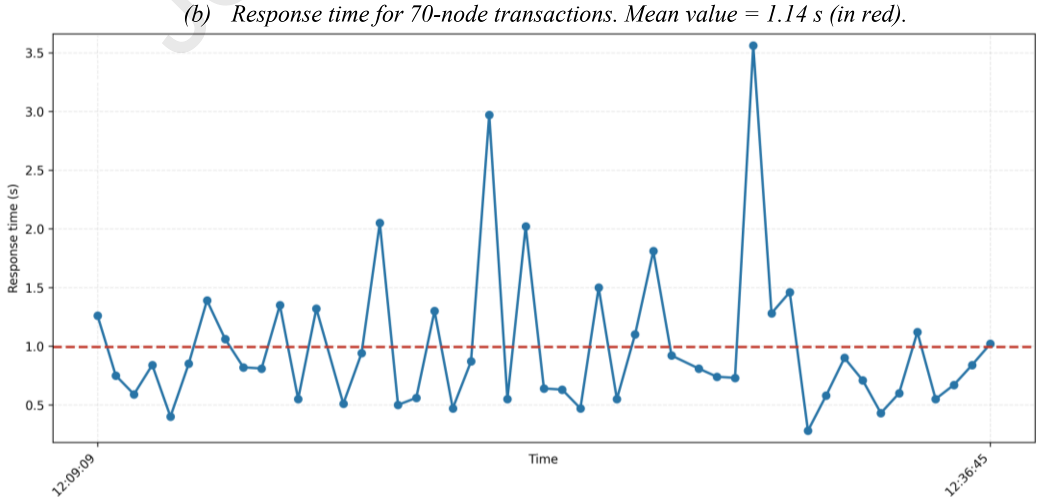

(c) Response time for 100-node transactions. Mean value = 0.99 s (in red).

Figure 7. Response time (in blue) from when data is published on The Things Network to when it is stored in IOTA for a) 50 nodes, b) 70 nodes and c) 100 nodes.

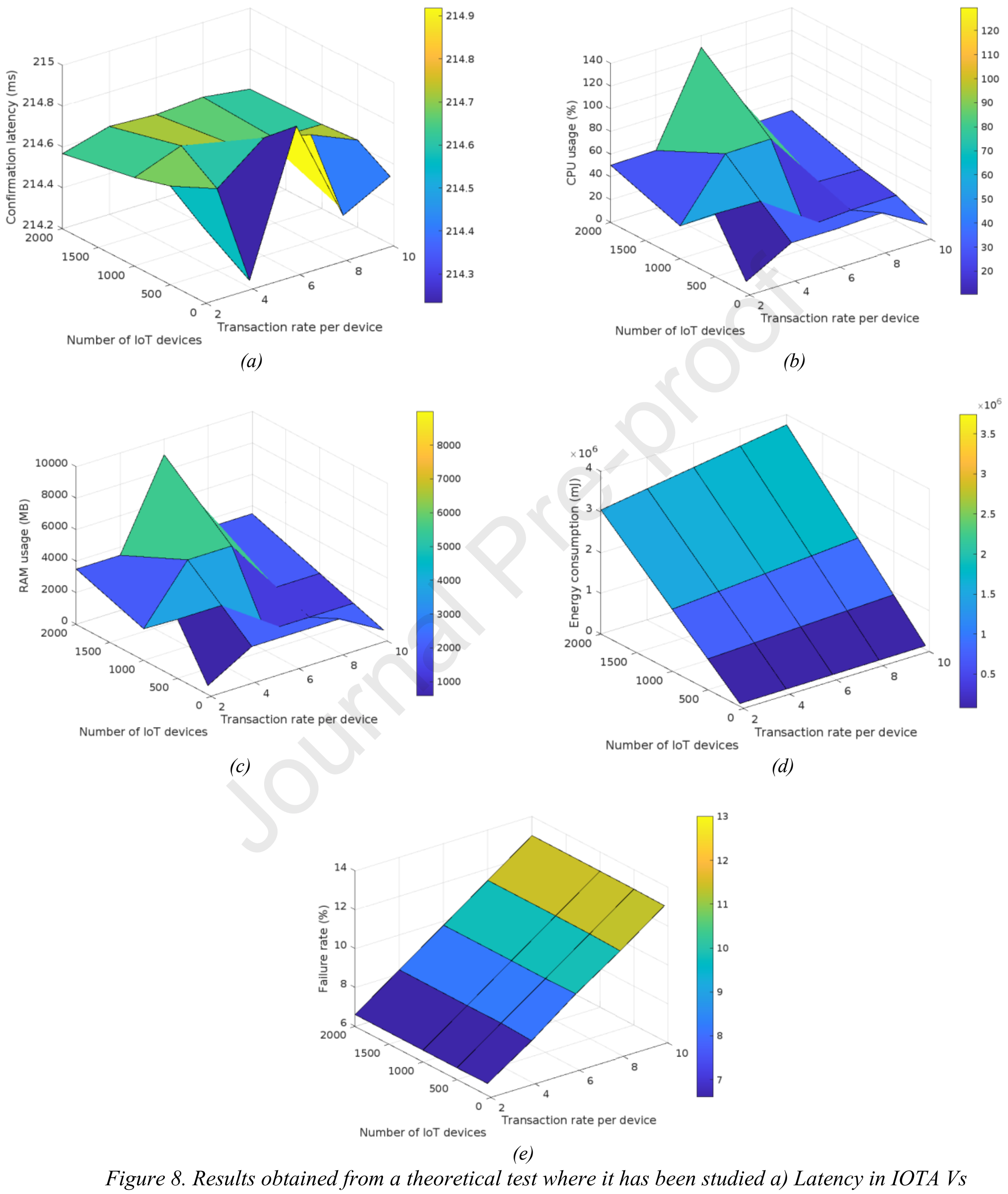

Figure 8. Results obtained from a theoretical test where it has been studied a) Latency in IOTA Vs Scalability, b) CPU Load in IOTA node, c) RAM Load in IOTA node, d) Energy consumption in the IoT system with IOTA and e) Impact of congestion in IOTA on board.

5. Discussion

The results show that IOTA is a viable solution for IoT systems in maritime environments, with transactions per second limited to 6 transactions per second per device due to its scalability (with up to 2000 devices), low transaction confirmation latency (around 214 ms), and energy efficiency. Additionally, the non-linear behavior observed in the scalability tests is a direct consequence of the probabilistic validation mechanism of the IOTA Tangle [45]. As the number of transactions and nodes increases, the tip selection algorithm requires additional computational effort to select and confirm unreferenced transactions, which introduces a variable proof-of-work time. Unlike blockchain systems with deterministic block intervals, the asynchronous structure of the Tangle allows multiple concurrent validations, leading to temporary network congestion and uneven propagation of confirmation times. This explains why latency and resource usage increase non-linearly with node density, even though the average confirmation time remains stable within operational limits. The results therefore reflect the self-regulating behavior of the DAG rather than scalability degradation.

In comparison with conventional commercial monitoring systems that rely on centralized cloud databases or proprietary middleware, the proposed architecture achieves similar or better latency values while removing the single point of failure inherent to centralized solutions [46]. Traditional LoRaWAN-based data loggers typically operate with end-to-end latencies above 1 s under moderate network loads and provide limited traceability once the data leave the gateway [45], [47], [48]. In contrast, the integration of IOTA enables average confirmation times below 250 ms while ensuring tamper-evident persistence through decentralized storage in the Tangle [49], [50]. From an operational standpoint, this represents an improvement over standard MQTT or HTTP-based implementations, where retransmission and authentication delays can dominate total response time. Furthermore, the proposed system achieves multi-month autonomy with minimal computational requirements, whereas commercial solutions offering similar connectivity and storage reliability generally depend on more expensive infrastructure and require frequent battery replacement.

5.1. Limitations

The proposed system presents limitations linked to the technology used for its design. Thus, although LoRa enables local onboard communications, it requires a satellite connectivity system to guarantee communications on the high seas. Currently, commercial systems, such as those offered by Starlink, Lecuna, Satelliot, or FOSSA Systems, exist to provide this service. Recent literature has also addressed the special characteristics of these systems [10]. Therefore, their design has not been studied in this work.

In this context, the ability to validate transactions in decentralized networks, such as the IOTA Tangle, can be restricted by latency and available bandwidth under high-load conditions [51], which are characteristic of environments, like large commercial ports. In these cases, network congestion affects not only transmission speed but also the ability of nodes to participate in distributed consensus, potentially delaying transaction confirmation. The network availability and performance must be evaluated considering the vessel's specific route, as coverage and link quality depend significantly on the geographic regions crossed. It is necessary to analyze the capabilities of the satellite operators involved in the implementation, including parameters such as average latency, data transfer rate, resilience to interruptions, and the time required to reestablish connections. These factors determine not only the viability of the proposed solution but also its robustness in the face of prolonged disconnection scenarios or congestion at high-density operating points.

Furthermore, LoRa has limited bandwidth [43]. Although it is sufficient for transmitting the parameters proposed in this work, transmitting a larger volume of information in real-time, such as images, is not feasible. Furthermore, an onboard LoRa network will require strategically placed gateways or repeaters on the vessel to ensure coverage. The design, number, and location of these elements have not been addressed explicitly in this work because they will depend on the construction characteristics of the vessel.

5.2. Future works

Future lines of research that emerge from this work are:

- *Validation of the system on long routes and extreme weather conditions:* This includes adapting and validating the system for different plant species, considering their specific transport needs, and analyzing their behaviour in environments with significant climate variability, such as high temperatures, high relative humidity, or strong thermal fluctuations.
- *Integration of predictive models based on Artificial Intelligence (AI): This* would allow for anticipating changes in internal and external environmental conditions during the maritime journey. Predictive models can analyze both historical and real-time data to optimize adjustment decisions, thereby improving the system's ability to prevent cargo damage and minimize the need for human intervention.
- *Strengthening data security:* This would involve utilising state-of-the-art encryption standards and robust authentication systems to mitigate the risk of cyberattacks in the maritime supply chain, thereby reinforcing trust in the handling of information.
- *Energy consumption optimization:* Future research can focus on integrating ultra-low-consumption hardware and more effectively managing data collection and transmission cycles.
- *Connection with global logistics chains:* This would enable data generated on the ship to be linked to other nodes in the supply chain, thereby improving transparency and coordination among actors.

6. Conclusions

This work presents the design, implementation, and evaluation of an IoT node for monitoring environmental parameters during the maritime transport of live plants. The system combines LoRa technology for intra-vessel communication with IOTA for decentralised and immutable data storage, ensuring continuous monitoring and enhancing transparency in the supply chain.

Experimental validation confirmed that the proposed node can accurately monitor ambient temperature, soil temperature, relative humidity, soil moisture, and luminosity within the tolerances specified by the sensors. Statistical analysis demonstrated that deviations from reference values were not significant under controlled maritime-like conditions, supporting the reliability of the collected data. Energy consumption tests showed that battery autonomy is compatible with extended maritime routes when sampling frequencies are properly adjusted. Scalability simulations further indicated that IOTA can handle increasing numbers of devices with acceptable latency, although congestion may occur under extreme transaction loads.

Despite these results, the system presents limitations. LoRa coverage in metal-rich maritime environments requires careful placement of gateways, and practical validation on vessels is still needed. Satellite integration, although feasible, depends on operator availability, latency, and cost factors that have not been exhaustively tested. Security claims regarding traceability and immutability are inherent to the IOTA Tangle; however, these were not complemented by penetration testing of the IoT nodes themselves. Additionally, long-term reliability studies covering multiple voyages and diverse plant species remain pending.

The cost model demonstrates that while hardware costs per node are relatively modest, the total cost of ownership depends significantly on maintenance (including sensor calibration and battery replacement) and operational expenses (such as satellite subscriptions, cloud hosting, and technical support). This highlights the importance of considering not only initial deployment costs but also lifecycle sustainability.

Future work will focus on large-scale validation in real maritime conditions, integration of predictive algorithms to anticipate cargo deterioration, strengthening of data security mechanisms, and connection with global logistics platforms to enhance interoperability.

6.1.1. Conflict of interest

The authors have no conflict of interest in publishing this work

6.1.2. Plagiarism

The work described has not been published previously (except in the form of an abstract or as part of a published lecture or academic thesis) and is not under consideration for publication elsewhere. No article with the same content will be submitted for publication elsewhere, that its publication is approved by all authors and tacitly or explicitly by the responsible authorities where the work was carried out, and that, if accepted, it will not be published elsewhere in the same form, in English or in any other language, without the written consent of the copyright-holder.

6.1.3. Declaration of generative AI and AI-assisted technologies in the writing process

During the preparation of this work the authors used Grammarly and ChatGPT in order to improve language and readability. After using this tool/service, the authors reviewed and edited the content as needed and takes full responsibility for the content of the publication.

6.1.4. Credit authorship contribution statement

Paula Lamo contributed to the conceptualization and methodological design of the study, coordinated the project administration, supervised all stages of the work, and participated in the validation of results. She also contributed to both the drafting of the original manuscript and the subsequent review and editing of its final version. Blanca Méndez was responsible for data curation and formal analysis, developed the software components and managed the technical resources required for the study, and participated in the validation process. She also prepared the visualizations and contributed to the drafting of the original manuscript. All authors have approved the final article to be true.

6.1.5. Data availability statement

The data that support the findings of this study are available in the Zenodo repository at the following DOI: https://doi.org/10.5281/zenodo.14979221

6.1.6. Declaration of competing interest

The authors declare that they have no competing financial or personal interests that could have appeared to influence the work reported in this paper.

7. References

[1] *E. Ferrari, P. Christidis, and P. Bolsi, "The impact of rising maritime transport costs on international trade: Estimation using a multi-region general equilibrium model," Transportation Research Interdisciplinary Perspectives, vol. 22, p. 100985, Nov. 2023, doi: 10.1016/j.trip.2023.100985.*

[2] *L. Shen, G. Zhu, X. Qian, L. Zhang, Y. Wang, and X. Shi, "Risk Analysis of Cold Logistics Chains in Maritime Transportation," in 2019 5th International Conference on Transportation Information and Safety (ICTIS), July 2019, pp. 1152–1162. doi: 10.1109/ICTIS.2019.8883747.*

[3] *N. Shaikh, K. Kasat, V. Moyal, N. D. Kumar, S. Ponnusamy, and K. Pavithra, "Application of IoT to Monitor the Shipping of Goods in Maritime Transportation System," in 2022 IEEE North Karnataka Subsection Flagship International Conference (NKCon), Nov. 2022, pp. 1–5. doi: 10.1109/NKCon56289.2022.10127075.*

[4] *P.-L. Sanchez-Gonzalez, D. Díaz-Gutiérrez, and L. R. Núñez-Rivas, "Digitalizing Maritime Containers Shipping Companies: Impacts on Their Processes," Applied Sciences, vol. 12, no. 5, Art. no. 5, Jan. 2022, doi: 10.3390/app12052532.*

[5] *M. Kalinowski, R. Koba, P. Lipka, K. Czaplewski, A. Weintrit, and J. Witkowska, "Exploring External Costs on the Example of Sea–Land Transport Chains of Refrigerated Cargo Between Spain and Poland," Sustainability, vol. 17, no. 1, Art. no. 1, Jan. 2025, doi: 10.3390/su17010162.*

[6] *L. Parri, S. Parrino, G. Peruzzi, and A. Pozzebon, "Low Power Wide Area Networks (LPWAN) at Sea: Performance Analysis of Offshore Data Transmission by Means of LoRaWAN Connectivity for Marine Monitoring Applications," Sensors, vol. 19, no. 14, Art. no. 14, Jan. 2019, doi: 10.3390/s19143239.*

[7] *J. Wang, Y. Xiao, T. Li, and C. L. P. Chen, "A Survey of Technologies for Unmanned Merchant Ships," IEEE Access, vol. 8, pp. 224461–224486, 2020, doi: 10.1109/ACCESS.2020.3044040.*

[8] *S. Ugale and A. Potgantwar, "Container Security in Cloud Environments: A Comprehensive Analysis and Future Directions for DevSecOps," Engineering Proceedings, vol. 59, no. 1, Art. no. 1, 2023, doi: 10.3390/engproc2023059057.*

[9] *Y. Ma, K. Liu, M. Chen, Y. Li, R. Sun, and R. Ranjan, "Rapid Crowd Evacuation for Passenger Ships Using LPWAN," IEEE Transactions on Intelligent Transportation Systems, vol. 25, no. 2, pp. 1720–1735, Feb. 2024, doi: 10.1109/TITS.2023.3314081.*

[10] *O. Ledesma, P. Lamo, and J. A. Fraire, "Trends in LPWAN Technologies for LEO Satellite Constellations in the NewSpace Context," Electronics, vol. 13, no. 3, Art. no. 3, Jan. 2024, doi: 10.3390/electronics13030579.*

[11] *J. A. Tagiltseva, E. L. Kuzina, M. A. Vasilenko, N. V. Babloyan, A. V. Vasilchenko, and A. M. Prokopova, "The Modeling Digital Transformation of the Regional Container Transportation Organization," in 2022 International Conference on Quality Management, Transport and Information Security, Information Technologies (IT&QM&IS), Sept. 2022, pp. 112–116. doi: 10.1109/ITQMIS56172.2022.9976712.*

[12] *I. Progoulakis, P. Rohmeyer, and N. Nikitakos, "Cyber Physical Systems Security for Maritime Assets," Journal of Marine Science and Engineering, vol. 9, no. 12, Art. no. 12, Dec. 2021, doi: 10.3390/jmse9121384.*

[13] *H. Han, A. Kan, and J. Ji, "Investigation of Monitor-and-Control Software of Marine Refrigerated Container," in 2009 International Forum on Computer Science-Technology and Applications, Dec. 2009, pp. 350–353. doi: 10.1109/IFCSTA.2009.355.*

[14] *N. Ayres, L. Deka, and D. Paluszczyszyn, "Container-Based Electronic Control Unit Virtualisation: A Paradigm Shift Towards a Centralised Automotive E/E Architecture," Electronics, vol. 13, no. 21, Art. no. 21, Jan. 2024, doi: 10.3390/electronics13214283.*

[15] *"Collaborative Optimization of Container Liner Slot Allocation and Empty Container Repositioning Based on Online Booking Platform." Accessed: Apr. 08, 2025. [Online]. Available: https://www.mdpi.com/2076-3417/14/23/11092*

[16] *S. Pullo, R. Pareschi, V. Piantadosi, F. Salzano, and R. Carlini, "Integrating IOTA's Tangle with the Internet of Things for Sustainable Agriculture: A Proof-of-Concept Study on Rice Cultivation," Informatics, vol. 11, no. 1, Art. no. 1, Mar. 2024, doi: 10.3390/informatics11010003.*

[17] I.-C. Lin, P.-C. Tseng, Y.-S. Chang, and T.-C. Weng, "IOTA Data Preservation Implementation for Industrial Automation and Control Systems," Processes, vol. 11, no. 7, Art. no. 7, July 2023, doi: 10.3390/pr11072160.

[18] M. F. M. S. Mustafa, N. Navaranjan, and A. Demirovic, "Food cold chain logistics and management: A review of current development and emerging trends," Journal of Agriculture and Food Research, vol. 18, p. 101343, Dec. 2024, doi: 10.1016/j.jafr.2024.101343.

[19] M. S. Yar, I. H. Ibeogu, A. Regmi, N. Zhang, and C. Li, "Advances in intelligent time-temperature indicators for cold chain monitoring: mechanisms, challenges, and applications," Trends in Food Science & Technology, vol. 163, p. 105128, Sept. 2025, doi: 10.1016/j.tifs.2025.105128.

[20] G. Franzoni, C. Rovera, S. Farris, and A. Ferrante, "Packaging materials and their effect on ruscus quality changes during storage and vase life," Postharvest Biology and Technology, vol. 210, p. 112789, Apr. 2024, doi: 10.1016/j.postharvbio.2024.112789.

[21] M. Zhang, Y. Han, D. Li, S. Xu, and Y. Huang, "Smart horticulture as an emerging interdisciplinary field combining novel solutions: Past development, current challenges, and future perspectives," Horticultural Plant Journal, vol. 10, no. 6, pp. 1257–1273, Nov. 2024, doi: 10.1016/j.hpj.2023.03.015.

[22] E. O. Olaniyi, M. C. Solarte-Vasquez, and T. Inkinen, "Smart regulations in maritime governance: Efficacy, gaps, and stakeholder perspectives," Marine Pollution Bulletin, vol. 202, p. 116341, May 2024, doi: 10.1016/j.marpolbul.2024.116341.

[23] "ISO 22005:2007," ISO. Accessed: Oct. 08, 2025. [Online]. Available: https://www.iso.org/standard/36297.html

[24] "Directive - 2014/53 - EN - EUR-Lex." Accessed: Oct. 08, 2025. [Online]. Available: https://eur-lex.europa.eu/eli/dir/2014/53/oj/eng

[25] S. Noto, M. Gharbaoui, M. Falcitelli, B. Martini, P. Castoldi, and P. Pagano, "Experimental Evaluation of an IoT-Based Platform for Maritime Transport Services," Applied System Innovation, vol. 6, no. 3, Art. no. 3, June 2023, doi: 10.3390/asi6030058.

[26] S. E. Elgharbi, M. Iturralde, Y. Dupuis, and A. Gaugue, "Maritime monitoring through LoRaWAN: Resilient decentralised mesh networks for enhanced data transmission," Computer Communications, vol. 241, p. 108276, Sept. 2025, doi: 10.1016/j.comcom.2025.108276.

[27] I. Karin, I. G. Medvešek, and J. Šoda, "Best-Suited Communication Technology for Maritime Signaling Facilities: A Literature Review," Applied Sciences, vol. 15, no. 7, p. 3452, Jan. 2025, doi: 10.3390/app15073452.

[28] O. Ledesma and P. Lamo, "Hybrid IoT network for real-time monitoring of maritime containers," Computer Networks, vol. 271, p. 111627, Oct. 2025, doi: 10.1016/j.comnet.2025.111627.

[29] Z. K. Idrissi, M. Lachgar, and H. Hrimech, "Blockchain, IoT and AI in logistics and transportation: A systematic review," Transport Economics and Management, vol. 2, pp. 275–285, Dec. 2024, doi: 10.1016/j.team.2024.09.002.

[30] M. Jovanovic, N. Kostić I. M. Sebastian, and T. Sedej, "Managing a blockchain-based platform ecosystem for industry-wide adoption: The case of TradeLens," Technological Forecasting and Social Change, vol. 184, p. 121981, Nov. 2022, doi: 10.1016/j.techfore.2022.121981.

[31] Z. Li and Y. Sun, "Blockchain in maritime: applications, effects and challenges," Front. Mar. Sci., vol. 12, July 2025, doi: 10.3389/fmars.2025.1627544.

[32] W. C. Quigley, M. Rahouti, and G. M. Weiss, "A Secure Blockchain-Assisted Framework for Real-Time Maritime Environmental Compliance Monitoring," Mar. 10, 2025, arXiv: arXiv:2503.08707. doi: 10.48550/arXiv.2503.08707.

[33] I. Ashraf et al., "A Survey on Cyber Security Threats in IoT-Enabled Maritime Industry," IEEE Transactions on Intelligent Transportation Systems, vol. 24, no. 2, pp. 2677–2690, Feb. 2023, doi: 10.1109/TITS.2022.3164678.

[34] D. Sudha, B. Unhelkar, S. Shankar, and G. Nagarajan, "Designing low-power encryption algorithms for end-to-end vehicular data protection in sustainable IoT networks," Results in Engineering, vol. 28, p. 107474, Dec. 2025, doi: 10.1016/j.rineng.2025.107474.

[35] U. Tatar, B. Karabacak, O. F. Keskin, and D. P. Foti, "Charting new waters with CRAMMTS: A survey-driven cybersecurity risk analysis method for maritime stakeholders," Computers & Security, vol. 145, p. 104015, Oct. 2024, doi: 10.1016/j.cose.2024.104015.

[36] T. Defraeye, C. Verreydt, J. Gonthier, L. Lukasse, P. Cronjé, and T. Berry, "Building a physics-based virtual refrigerated container filled with fruit in ventilated packaging," MethodsX, vol. 13, p. 102984, Dec. 2024, doi: 10.1016/j.mex.2024.102984.

[37] "THE INFLUENCE OF TIME AND TEMPERATURE DURING SIMULATED SHIPMENT ON THE QUALITY OF POT PLANTS | International Society for Horticultural Science." Accessed: Oct. 06, 2025. [Online]. Available: http://www.actahort.org/books/181/181_60.htm

[38] A. J. Both et al., “Guidelines for measuring and reporting environmental parameters for experiments in greenhouses,” Plant Methods, vol. 11, no. 1, p. 43, Sept. 2015, doi: 10.1186/s13007-015-0083-5.

[39] H. Nishi, Y. Takayama, J. L. Wijekoon, E. Y. Song, and K. B. Lee, “Temperature Monitoring and Airflow Control System for Balancing the Greenhouse Environment Using IEEE 1451 Standards,” in IECON 2023- 49th Annual Conference of the IEEE Industrial Electronics Society, Oct. 2023, pp. 1–6. doi: 10.1109/IECON51785.2023.10312312.

[40] J. H. Jeong and W. Oh, “Drought and Darkness during Long-Term Simulated Shipping Delay Post-Shipping Flowering of Phalaenopsis Sogo Yukidian ‘V3,’” Horticulturae, vol. 7, no. 11, p. 483, Nov. 2021, doi: 10.3390/horticulturae7110483.

[41] F. Abbas et al., “Comprehensive Review on Evaporative Cooling and Desiccant Dehumidification Technologies for Agricultural Greenhouses,” AgriEngineering, vol. 7, no. 7, p. 222, July 2025, doi: 10.3390/agriengineering7070222.

[42] S. E. Elgharbi, M. Iturralde, Y. Dupuis, and A. Gaugue, “Maritime monitoring through LoRaWAN: Resilient decentralised mesh networks for enhanced data transmission,” Computer Communications, vol. 241, p. 108276, Sept. 2025, doi: 10.1016/j.comcom.2025.108276.

[43] H. Zeng, K. Yang, J. Wu, J. Ding, C. Wen, and X. Li, “LoRa Path-Loss Model and Verification for Maritime Environment,” in 2023 IEEE International Conference on Unmanned Systems (ICUS), Oct. 2023, pp. 1587–1591. doi: 10.1109/ICUS58632.2023.10318285.

[44] J. Zhang, H. Liu, Y. He, W. Gao, N. Xu, and C. Liu, “MCLORA: Maritime ad-hoc communication system based on LORA,” High-Confidence Computing, vol. 5, no. 3, p. 100275, Sept. 2025, doi: 10.1016/j.hcc.2024.100275.

[45] M. Alshaikhli, S. Al-Maadeed, and M. Saleh, “Enhancing Scalability and Network Efficiency in IOTA Tangle Networks: A POMDP-Based Tip Selection Algorithm,” Computers, vol. 14, no. 4, p. 117, Apr. 2025, doi: 10.3390/computers14040117.

[46] S. M. Alrubei, E. A. Ball, J. M. Rigelsford, and Callum. A. Willis, “Latency and Performance Analyses of Real-World Wireless IoT-Blockchain Application,” IEEE Sensors Journal, vol. 20, no. 13, pp. 7372–7383, July 2020, doi: 10.1109/JSEN.2020.2979031.

[47] M. Jouhari, N. Saeed, M.-S. Alouini, and E. M. Amhoud, “A Survey on Scalable LoRaWAN for Massive IoT: Recent Advances, Potentials, and Challenges,” IEEE Communications Surveys & Tutorials, vol. 25, no. 3, pp. 1841–1876, 2023, doi: 10.1109/COMST.2023.3274934.

[48] D. Tamang, A. Pozzebon, L. Parri, A. Fort, and A. Abrardo, “Designing a Reliable and Low-Latency LoRaWAN Solution for Environmental Monitoring in Factories at Major Accident Risk,” Sensors, vol. 22, no. 6, p. 2372, Jan. 2022, doi: 10.3390/s22062372.

[49] M. Alshaikhli, S. Al-Maadeed, and M. Saleh, “Enhancing Scalability and Network Efficiency in IOTA Tangle Networks: A POMDP-Based Tip Selection Algorithm,” Computers, vol. 14, no. 4, p. 117, Apr. 2025, doi: 10.3390/computers14040117.

[50] A. Rawat, V. Daza, and M. Signorini, “Offline Scaling of IoT Devices in IOTA Blockchain,” Sensors, vol. 22, no. 4, p. 1411, Jan. 2022, doi: 10.3390/s22041411.

[51] A. Kumari and I. Sharma, “Augmentation of Internet of Things Security and Privacy with IOTA Tangle Network,” in 2023 4th IEEE Global Conference for Advancement in Technology (GCAT), Oct. 2023, pp. 1–5. doi: 10.1109/GCAT59970.2023.10353394.

Highlights:

- Turns maritime containers into smart greenhouses for resilient plant transport
- Validates continuous maritime IoT via combined LoRa links and LEO connectivity
- Provides immutable end-to-end traceability through IOTA Tangle integration
- Validates accuracy, stability and energy efficiency through controlled 30-day tests

Declaration of interests

☒ The authors declare that they have no known competing financial interests or personal relationships that could have appeared to influence the work reported in this paper.

☐ The authors declare the following financial interests/personal relationships which may be considered as potential competing interests: